 https://ieeexplore.ieee.org/document/8795828

DOI: 10.23919/ECC.2019.8795828

Moving Horizon Demand and State Estimation for Model Predictive Perimeter Control of Large-scale Urban Networks

Isik Ilber Sirmatel and Nikolas Geroliminis

***Abstract*— Perimeter control schemes proposed to alleviate congestion in large-scale urban networks usually assume perfect knowledge of the accumulation state and inflow demands, both requiring information about the origins and destinations of drivers. Such assumptions are problematic for practice due to measurement noise and difficulty of obtaining OD-based information. We address these by a nonlinear moving horizon estimation (MHE) scheme for the combined demand and state estimation for a two region large-scale urban road network with dynamics described via macroscopic fundamental diagram. We consider various measurement configurations likely to be encountered in practice, such as measurements on regional accumulations and transfer flows without OD information, and provide results of their observability tests. A model predictive perimeter control scheme is combined with the MHE to present an application case. Simulation studies demonstrate operation of the proposed scheme.**

I. INTRODUCTION

Modeling, estimation, and control of large-scale urban road networks present considerable challenges. Inadequate infrastructure and coordination, low sensor coverage, spatiotemporal propagation of congestion, and the uncertainty in traveler choices contribute to the difficulties faced when creating realistic models and designing effective estimation and control schemes for urban networks. Although considerable research has focused on real-time traffic control in the last decades, estimation and control of heterogeneously congested large-scale networks remains a challenging problem.

Studies on traffic modeling and control for urban networks usually focus on microscopic models keeping track of link-level traffic dynamics with control strategies using local information. Based on the linear-quadratic regulator (LQR) problem, traffic-responsive urban control (TUC) [1] and its extensions (see [2], [3]) represent a multivariable feedback regulator approach for network-wide urban traffic control. Although TUC can deal with oversaturated conditions via minimizing and balancing the relative occupancies of network links, it may not be optimal for heterogeneous networks with multiple pockets of congestion. Inspired by the max pressure routing scheme for wireless networks, many local traffic control schemes have been proposed for networks of signalized intersections (see [4], [5], [6], [7]), which involve evaluations at each intersection requiring information exclusively from adjacent links. Although the high accuracy of microscopic traffic models is desirable for simulation purposes, the increased model complexity results in complications for control, whereas local control strategies might not be able to operate properly under heavily congested conditions and fast propagation, as they do not protect the congested regions upstream. Another disadvantage of sophisticated local controllers is that they might require detailed information on traffic states, which is difficult to estimate or measure.

Literature on state estimation for road traffic focuses mainly on freeway networks: A mixture Kalman filter based on the cell transmission model is proposed in [8]. In [9], an extended Kalman filter is designed for real-time state and parameter estimation for a freeway network with dynamics described by the METANET model [10]. A particle filtering framework is proposed in [11] for a second order freeway traffic model that is efficiently parallelizable. Superiority of Lagrangian state estimation formulations over the Eulerian case using extended Kalman filters for the Lighthill-Whitham and Richards (LWR) model is reported in [12]. There is also some literature on urban traffic state estimation: In [13] an unscented Kalman filter is designed based on a kinematic wave model modified for urban traffic. An approach integrating the Kalman filter with advanced data fusion techniques is taken by [14] for urban network state estimation. A data fusion based extended Kalman filter is proposed in [15] for urban corridors based on the LWR model. Interestingly, even though there is considerable literature on traffic state estimation (especially for freeways), there are not many works on comparable techniques for large-scale urban networks.

An alternative to local traffic control methods is the hierarchical approach. At the upper layer, a network-level controller optimizes network performance via regulating macroscopic traffic flows through interregional actuation systems (e.g., perimeter control), whereas at the lower layer the local controllers regulate microscopic traffic movements through intraregional actuation systems (e.g., signalized intersections). The macroscopic fundamental diagram (MFD) of urban traffic is a modeling tool for developing aggregated dynamic models of urban networks, which are required for the design of efficient network-level control schemes for the upper layer. It is possible to model an urban region with roughly homogeneous accumulation (i.e., small spatial link density heterogeneity) with an MFD, which provides a unimodal, low-scatter, and demand-insensitive relationship between accumulation and trip completion flow (see [16]).

The concept of MFD with an optimal accumulation was

This research has been supported by the ERC (European Research Council) Starting Grant "METAFERW: Modeling and controlling traffic congestion and propagation in large-scale urban multimodal networks" (Grant # 338205).

The authors are with Urban Transport Systems Laboratory, School of Architecture, Civil & Environmental Engineering, École Polytechnique Fédérale de Lausanne, 1015 Lausanne, Switzerland. {isik.sirmatel,nikolas.geroliminis}@epfl.ch

first proposed in [17], and its existence was recently verified with dynamic features and real data in [16]. Control strategies based on MFD modeling using perimeter control type actuation (i.e., manipulating transfer flows between neighboring regions) have been proposed by many researchers (see [18], [19], [20], [21], [22], [23], [24], [25]). Application of the MPC technique to the control of urban networks with MFD modeling also attracted recent interest. As the first work on this direction, in [26] a nonlinear MPC is designed for a two-region network actuated with perimeter control. The study in [27] suggests hybrid MPC schemes integrating perimeter control and switching signal timing plans. A model capturing the dynamics of heterogeneity is proposed in [28] together with a hierarchical control scheme with MPC on the upper level. An integration of perimeter control and route guidance type actuation within an MPC framework is developed in [29]. A more detailed literature review of MFD-based modeling and control can be found in [30].

Most works on perimeter control assume that: a) Accumulations $n_{ij}(t)$ are known (i.e., measured perfectly), b) future inflow demands $q_{ij}(t)$ are available. Such assumptions are problematic for practice due to following reasons: 1) Measurements are corrupted by noise, 2) measuring $n_{ij}(t)$ or $q_{ij}(t)$ is difficult as they require information on the origins and destination of drivers, 3) assuming known future values of $q_{ij}(t)$ is unrealistic. We address the first two points in this paper by a nonlinear moving horizon estimation (MHE) scheme capable of combined demand and state estimation.

II. Modeling

Consider a heterogeneous urban road network that can be partitioned into 2 homogeneous regions. Each region i, $i \in \{1, 2\}$, has a well-defined outflow MFD, defined via $G_i(n_i(t))$ (veh/s), which is the outflow (i.e., trip completion flow) at accumulation $n_i(t)$. The flow of vehicles appearing in region i and demanding trips to destination j (i.e., origin-destination (OD) inflow demand) is $q_{ij}(t)$ (veh/s), whereas $n_{ij}(t)$ (veh) is the accumulation in region i with destination j, while $n_i(t)$ (veh) is the regional accumulation at time t; $n_i(t) = \sum_{j=1}^{2} n_{ij}(t)$. Between the two regions there exists perimeter control actuators, modeled via the control inputs $u_{12}(t)$ and $u_{21}(t) \in [0, 1]$, that can manipulate the transfer flows. Dynamics of a 2-region MFDs network is [26]:

$$\dot{n}_{11}(t) = q_{11}(t) + M_{21}(t) - M_{11}(t) \tag{1a}$$
$$\dot{n}_{12}(t) = q_{12}(t) - M_{12}(t) \tag{1b}$$
$$\dot{n}_{21}(t) = q_{21}(t) - M_{21}(t) \tag{1c}$$
$$\dot{n}_{22}(t) = q_{22}(t) + M_{12}(t) - M_{22}(t), \tag{1d}$$

while $M_{ii}(t)$ and $M_{ij}(t)$ express the exit (i.e., vehicles disappearing from the network) and transfer flows (i.e., vehicles transferring between regions), respectively:

$$M_{ii}(t) = \frac{n_{ii}(t)}{n_i(t)} G_i(n_i(t)) \quad \forall i \in \{1, 2\} \tag{2a}$$
$$M_{ij}(t) = u_{ij}(t) \frac{n_{ij}(t)}{n_i(t)} G_i(n_i(t)) \quad \forall i \in \{1, 2\},\ j \neq i. \tag{2b}$$

All trips inside a region are assumed to have similar trip lengths (i.e., the origin and destination of the trip does not affect the distance traveled by a vehicle). Simulation and empirical results [16] suggest the possibility of approximating the MFD by an asymmetric unimodal curve skewed to the right (i.e., the critical accumulation n_i^{cr}, for which $G_i(n_i(t))$ is at maximum, is less than half of the jam accumulation n_i^{jam} that puts the region in gridlock). Thus, $G_i(n_i(t))$ can be expressed using a third degree polynomial in $n_i(t)$:

$$G_i(n_i(t)) = a_i n_i^3(t) + b_i n_i^2(t) + c_i n_i(t), \tag{3}$$

where a_i, b_i, and c_i are known parameters (which are to be estimated from historical data in practice).

III. Optimal Estimation and Control

A. Modeling for Demand Estimation

For purposes of OD inflow demand estimation, we model the inflow demands $q_{ij}(t)$ as parameters that are unknown but constant in time, augmenting the state with the demand terms, yielding the augmented dynamical system:

$$\begin{bmatrix} \dot{x}_n(t) \\ \dot{x}_q(t) \end{bmatrix} = \begin{bmatrix} f_n(x_n(t), x_q(t), u(t)) \\ \mathbf{0} \end{bmatrix}, \tag{4}$$

where $x_n(t)$ contains the accumulations $n_{ij}(t)$

$$x_n(t) = [n_{11}(t)\ n_{12}(t)\ n_{21}(t)\ n_{22}(t)]^{\mathrm{T}}, \tag{5}$$

$x_q(t)$ contains the inflow demands $q_{ij}(t)$

$$x_q(t) = [q_{11}(t)\ q_{12}(t)\ q_{21}(t)\ q_{22}(t)]^{\mathrm{T}}, \tag{6}$$

$u(t)$ contains the control inputs

$$u(t) = [u_{12}(t)\ u_{21}(t)]^{\mathrm{T}}, \tag{7}$$

whereas $f_n(\cdot)$ is the dynamics given in eq. (1), while $\mathbf{0}$ is a vector of zeros (expressing that the inflow demand terms are assumed to be constant in time, i.e., $\dot{q}_{ij}(t) = 0$).

Assuming access to measurement $y(t)$ corrupted by noise $v(t)$, we can write the dynamics and measurement as:

$$\dot{x}(t) = f(x(t), u(t)) + w(t) \tag{8}$$
$$y(t) = h(x(t), u(t)) + v(t) \tag{9}$$

where $x(t)$ is the augmented state

$$x(t) = [x_n(t)\ x_q(t)]^{\mathrm{T}}, \tag{10}$$

$f(\cdot)$ is the augmented dynamical system given in eq. (4), $h(\cdot)$ is the measurement equation, while $w(t)$ contains unknown disturbances used to account for plant-model mismatch:

$$\begin{aligned} w(t) &= [w_n(t)\ w_q(t)]^{\mathrm{T}} \\ w_n(t) &= [w_{n_{11}}(t)\ w_{n_{12}}(t)\ w_{n_{21}}(t)\ w_{n_{22}}(t)]^{\mathrm{T}} \\ w_q(t) &= [w_{q_{11}}(t)\ w_{q_{12}}(t)\ w_{q_{21}}(t)\ w_{q_{22}}(t)]^{\mathrm{T}}, \end{aligned} \tag{11}$$

where $w_{n_{ij}}(t) \sim \mathcal{N}(0, \sigma_{w_n}^2)$ and $w_{q_{ij}}(t) \sim \mathcal{N}(0, \sigma_{w_q}^2)$ are white Gaussian noise terms modeling disturbances in the accumulation dynamics and unknown variations of inflow demands, respectively.

B. Measurement Configurations

Measurements available in an application dictate which state variables can be included in the dynamical model used in the design of estimation and control schemes. In this section we present some measurement configurations likely to be encountered in large-scale urban road network management. The important question of whether the traffic state can be determined from available measurements (i.e., observability) will be tackled in the next section.

1) Measurements on Accumulations $n_{ij}(t)$: One straightforward measurement configuration involves simply measuring all accumulations $n_{ij}(t)$:

$$y_A(t) = h_A(x(t)) + v_A(t) \tag{12}$$

$$h_A(x(t)) = x_n(t), \tag{13}$$

where $v_A(t)$ is the vector of measurement noise terms associated with measurements of $n_{ij}(t)$:

$$v_A(t) = [v_{n_{11}}(t)\ v_{n_{12}}(t)\ v_{n_{21}}(t)\ v_{n_{22}}(t)]^{\mathrm{T}}, \tag{14}$$

where $v_{n_{ij}}(t) \sim \mathcal{N}(0, \sigma^2_{v,n_{ij}})$ is white Gaussian noise modeling sensor noise in the measurement of $n_{ij}(t)$. Knowing $n_{ij}(t)$ in real-time requires having drivers report their destination in the beginning of the trip, which is currently not straightforward to achieve.

2) Measurement on Regional Accumulations $n_i(t)$ and Transfer Flows $M_{ij}(t)$: As regional accumulations $n_i(t)$ and transfer flows $M_{ij}(t)$ can be easily measured with loop detectors (dispersed inside a region for $n_i(t)$ and placed at the boundary between regions for $M_{ij}(t)$), a more practical configuration involves measuring $M_{ij}(t)$ and $n_i(t)$:

$$y_B(t) = h_B(x(t), u(t)) + v_B(t)$$

$$h_B(x(t), u(t)) = \begin{bmatrix} n_1(t) \\ n_2(t) \\ M_{12}(t) \\ M_{21}(t) \end{bmatrix} \quad v_B(t) = \begin{bmatrix} v_{n_1}(t) \\ v_{n_2}(t) \\ v_{M_{12}}(t) \\ v_{M_{21}}(t) \end{bmatrix}, \tag{15}$$

where $v_{n_i}(t) \sim \mathcal{N}(0, \sigma^2_{v,n_i})$ and $v, M_{ij}(t) \sim \mathcal{N}(0, \sigma^2_{v_{M_{ij}}})$ are white Gaussian noise terms modeling sensor noise in the measurement of $n_i(t)$ and $M_{ij}(t)$, respectively.

3) Measurements on Inflow Demands $q_{ij}(t)$: In some well-instrumented applications it might be possible to measure all $q_{ij}(t)$ terms (or know them based on historical data with some uncertainty):

$$y_C(t) = h_C(x(t)) + v_C(t) \tag{16}$$

$$h_C(x(t)) = x_q(t), \tag{17}$$

where $v_C(t)$ is the vector of measurement noise terms associated with measurements of $q_{ij}(t)$:

$$v_C(t) = [v_{q_{11}}(t)\ v_{q_{12}}(t)\ v_{q_{21}}(t)\ v_{q_{22}}(t)]^{\mathrm{T}}, \tag{18}$$

where $v_{q_{ij}}(t) \sim \mathcal{N}(0, \sigma^2_{v,q_{ij}})$ is white Gaussian noise modeling sensor noise in the measurement of $q_{ij}(t)$.

4) Measurements on Regional Inflow Demands $q_i(t)$: Some applications might involve access to measurements on $q_i(t)$ instead of $q_{ij}(t)$ (e.g., when GPS information is collected for a sample of vehicles):

$$y_D(t) = h_D(x(t)) + v_D(t)$$

$$h_D(x(t)) = \begin{bmatrix} q_{11}(t) + q_{12}(t) \\ q_{21}(t) + q_{22}(t) \end{bmatrix} \quad v_D(t) = \begin{bmatrix} v_{q_1}(t) \\ v_{q_2}(t) \end{bmatrix}, \tag{19}$$

where $v_{q_i}(t) \sim \mathcal{N}(0, \sigma^2_{v,q_i})$ is white Gaussian noise modeling sensor noise in the measurement of $q_i(t)$.

C. Measurement Compositions and Observability Test

Availability of measurements affects observability of a dynamical system. Roughly stated, observability is about whether the state can be uniquely determined based on the measurements or not. A dynamical system (i.e., $f(\cdot)$ and $h(\cdot)$) has to be observable in order to do estimation. Observability of nonlinear systems can be checked using the *observability rank condition* developed in [31]. For affine-input systems (such as eq. (4)), which can be written in the following form:

$$\dot{x}(t) = f(x) + \sum_{j=1}^{m} g_j(x(t))u_j(t) \tag{20}$$

$$y_i(t) = h_i(x(t)),\ i = 1, \ldots, p, \tag{21}$$

where $x \in \mathbb{R}^l$ is the state, $u_j \in \mathbb{R}$ (with $j = 1, \ldots, m$) are control inputs, and $y_i \in \mathbb{R}$ (with $i = 1, \ldots, p$) are the measurements, it is possible to use a simpler form of the rank condition, as included in the software package developed in [32] or presented in an algorithm given in [33]. This observability test involves constructing the *observability codistribution* [32]:

$$\Omega_O = \langle f, g_1, \ldots, g_m \mid \text{span}\{dh_1, \ldots, dh_p\} \rangle, \tag{22}$$

and checking its rank. If the rank of Ω_O is equal to l (i.e., dimension of the state x), then the observability rank condition is satisfied [32], [33], indicating that the system is locally weakly observable (see §3 in [31] for details).

To check observability for our case, we conducted tests for the four measurement compositions based on combinations of the configurations given earlier:

$$h_1 = \begin{bmatrix} h_A \\ h_C \end{bmatrix}\ h_2 = \begin{bmatrix} h_A \\ h_D \end{bmatrix}\ h_3 = \begin{bmatrix} h_B \\ h_C \end{bmatrix}\ h_4 = \begin{bmatrix} h_B \\ h_D \end{bmatrix}. \tag{23}$$

Observability tests are done using the ProPac package [32] of the computer algebra tool Mathematica, where observability rank condition is checked for the dynamics eq. (4) and each measurement composition. In all four cases the system is locally weakly observable (see §3 in [31] for details).

Since measurement configurations involving limited or no OD-based information (i.e., h_2, h_3, and h_4) still yield observability, it is possible to design state estimators to reconstruct $n_{ij}(t)$ and $q_{ij}(t)$ from measurements, enabling development of traffic control schemes (combined with a state estimator) involving feedback on $n_{ij}(t)$ and $q_{ij}(t)$ even if these cannot be measured. This has important implications, as in practice $n_{ij}(t)$ and $q_{ij}(t)$ are difficult to measure.

D. Moving Horizon Estimation

We formulate the problem of finding state estimate trajectories for a moving time horizon extending a fixed length into the past, striking a trade-off between measurements and the prediction model, as the following MHE problem:

$$\begin{aligned}
\underset{x,w}{\text{minimize}} \quad & \sum_{k=0}^{N_\text{e}-1} \|w_k\|_Q^2 + \sum_{k=0}^{N_\text{e}} \|v_k\|_R^2 \\
\text{subject to} \quad & \text{for } k = 0, \dots, N_\text{e}: \\
& \quad v_k = y(t - N_\text{e} + k) - h(x_k, u_k) \\
& \text{for } k = 0, \dots, N_\text{e} - 1: \\
& \quad x_{k+1} = F(x_k, u(t - N_\text{e} + k), w_k, T) \\
& \text{for } k = 1, \dots, N_\text{e}: \\
& \quad \text{a) } 0 \le n_{ij,k} \quad \forall i,j \in \{1,2\} \\
& \quad \text{b) } n_{i,k} \le n_i^\text{jam} \quad \forall i \in \{1,2\} \\
& \quad \text{c) } 0 \le q_{ij,k} \le \bar{q}_{ij} \quad \forall i,j \in \{1,2\}
\end{aligned} \tag{24}$$

where k is the time interval counter internal to the MHE, N_e is the horizon of the MHE, t is the current time step, Q and R are weighting matrices on the disturbance and measurement noise, respectively, w_k, v_k, x_k, and u_k are the disturbance, measurement noise, state, and control input vectors, for the time interval k, respectively, h is the measurement equation, F is the discrete-time version of the dynamics given in eq. (8) with sampling time T, whereas $y(t)$ and $u(t)$ are measurement and control input vectors recorded at time step t, respectively, while $n_{ij,k}$, $n_{i,k}$, and $q_{ij,k}$ are the accumulation, regional accumulation, and inflow demand state variables internal to the MHE, respectively, with the constraints expressing their physical or known limits: a) accumulations are non-negative, b) regional accumulations cannot exceed jam accumulation, c) inflow demands are non-negative and cannot exceed some known upper bound $\bar{q}_{ij}$.

E. Model Predictive Control

We formulate the problem of finding the control inputs that minimize total time spent (TTS) for a finite horizon as the following MPC problem:

$$\begin{aligned}
\underset{u_k}{\text{minimize}} \quad & T \cdot \sum_{k=0}^{N_\text{c}} \sum_{i=1}^{2} \sum_{j=1}^{2} n_{ij,k} \\
\text{subject to} \quad & x_0 = \hat{x}(t) \\
& \text{for } k = 0, \dots, N_\text{c} - 1: \\
& \quad x_{k+1} = F(x_k, u_k, 0, T) \\
& \quad u_\text{min} \le u_k \le u_\text{max} \\
& \quad |u_0 - u(t-1)| \le \Delta_u \\
& \text{for } k = 1, \dots, N_\text{c}: \\
& \quad 0 \le n_{ij,k} \quad \forall i \in \{1,2\} \\
& \quad n_{i,k} \le n_{i,\text{jam}} \quad \forall i \in \{1,2\},
\end{aligned} \tag{25}$$

where k is the time interval counter internal to the MPC, N_c is the horizon of the MPC (i.e., the prediction horizon), $\hat{x}(t)$ is the available information (either measured or estimated) on the state $x(t)$ at time t (with t being the current time step), x_k and u_k are state and control input vectors internal to the MPC, respectively, F is the discrete-time version of the dynamics given in eq. (1) with sampling time T (with unknown disturbances w_k assumed to be 0), Δ_u is the rate limiting parameter on control inputs, whereas $n_{i,k}$ is the regional accumulation state variable internal to the MPC. Notice that this MPC scheme requires no information on future values of $q_{ij}(t)$, according to the prediction model the inflow demand terms are assumed to be fixed to their measured (or estimated) value contained in $\hat{x}(t)$ for the duration of the prediction horizon. Although this is not fully realistic, it is more practically reasonable compared to previously proposed model predictive perimeter control schemes assuming future $q_{ij}(t)$ values to be known.

The optimization problems given in eq. (24) and eq. (25) are nonconvex nonlinear programs, which can be solved efficiently via, e.g., sequential quadratic programming or interior point solvers (for details, see [34]).

IV. Simulation Results

A. Congested Scenario

In the congested scenario the network is uncongested at the beginning and faces increased inflow demands as time progresses. All simulations are conducted on a 2-region urban network with the simulation model given in eq. (8) for representing the reality. The regions have the same MFD, with the parameters $a_i = 4.133 \cdot 10^{-11}$, $b_i = -8.282 \cdot 10^{-7}$, $c_i = 0.0042$, jam accumulation $n_{i,\text{jam}} = 10^4$ (veh), critical accumulation $n_{i,\text{cr}} = 3.4 \cdot 10^3$ (veh), maximum outflow $G(n_{i,\text{cr}}) = 6.3$ (veh/s), for $i = \{1,2\}$, which are consistent with the MFD observed in downtown Yokohama (see [16]).

The MHE and MPC schemes are built using direct multiple shooting [35], with dynamics discretized via Runge–Kutta method with a timestep of $T = 90$ s. The implementation is done using MPCTools [36] (an interface to CasADi [37]) with IPOPT [38] as solver. Horizons are $N_\text{e} = N_\text{c} = 20$, following the tuning results of a study with the same network setup [26]. Control inputs are bounded as $0.1 \le u_{ij}(t) \le 0.9$, with a rate limit of $\Delta_u = 0.1$. Simulation length corresponds to 3.5 hours of real time.

Standard deviations of the process and measurement noise are chosen as $\sigma_{w_n} = 0.5$ veh/s, $\sigma_{v,n_{ij}} = 1000$ veh, $\sigma_{v,q_{ij}} = 0.5$ veh/s, $\sigma_{v,n_i} = 1000$ veh, $\sigma_{v,M_{ij}} = 1$ veh/s, $\sigma_{v,q_i} = 0.5$ veh/s, specifying severe noise and disturbance conditions. Weighting matrices of the MHE (i.e., Q and R) contain the inverses of these values, to reflect the fact that the stage cost terms related to the process and measurement noises should be weighted inversely proportional to the associated amount of uncertainty (that is, e.g., the measurements should be trusted more if the measurement noise has a lower variance).

Control performance is evaluated using TTS (veh.s), defined for a single simulation experiment as:

$$\text{TTS} = T \cdot \sum_{t=1}^{t_\text{final}} \sum_{i=1}^{2} \sum_{j=1}^{2} n_{ij}(t), \tag{26}$$

while for estimation performance we define two metrics based on the root-mean-square estimation error, one for $n_{ij}(t)$ and the other for $q_{ij}(t)$:

$$\text{RMSE}_n = \frac{1}{4}\sum_{i=1}^{2}\sum_{j=1}^{2}\sqrt{\frac{\sum_{t=1}^{t_{\text{final}}}(n_{ij}(t)-\hat{n}_{ij}(t))^2}{t_{\text{final}}}} \quad (27)$$

$$\text{RMSE}_q = \frac{1}{4}\sum_{i=1}^{2}\sum_{j=1}^{2}\sqrt{\frac{\sum_{t=1}^{t_{\text{final}}}(q_{ij}(t)-\hat{q}_{ij}(t))^2}{t_{\text{final}}}} \quad (28)$$

where $\hat{n}_{ij}(t)$ and $\hat{q}_{ij}(t)$ are the estimates computed by the MHE at time t, for $n_{ij}(t)$ and $q_{ij}(t)$, respectively.

A summary of the results is given in table I, which shows the TTS, RMSE_n, and RMSE_q values alongside the mean and maximum CPU times taken by the combined MHE-MPC scheme at a time step, for a no control case (with $u_{ij}(t)$ fixed to 0.9) and the four combined MHE-MPC schemes each with a different measurement composition as given in eq. (23). The results indicate that the proposed scheme, with all four compositions, is able to perform well even in the face of severe measurement noise. It is important to note here that a fair quantitative comparison between the four measurement compositions is impossible simply because they involve different measurements, the noise levels of which are not comparable. Furthermore, fig. 1 shows true, measured, and estimated values of accumulation $n_{12}(t)$ and inflow demand $q_{12}(t)$, for the MHE-MPC schemes with the four different measurement compositions. As expected, the cases with limited measurements on the inflows (i.e., h_2 and h_4) experience degraded estimation performance especially for $q_{ij}(t)$, while the most limited measurement case (i.e., h_4) has the most severe degradation.

B. Sensitivity to Measurement Noise Intensity

The effect of changing noise intensity on estimation performance is examined by a sensitivity analysis, where a set of 50 randomly generated scenarios is tested varying only the standard deviations of measurement noise: $\sigma_{v_{n_{ij}}}$ from 100 veh to 1000 veh for the h_1 and h_2 cases; $\sigma_{v_{n_i}}$ from 100 veh to 1000 veh and $\sigma_{v_{M_{ij}}}$ from 0.1 veh/s to 1 veh/s ($\sigma_{v_{n_i}}$ and $\sigma_{v_{M_{ij}}}$ changed together) for the h_3 and h_4 cases.

The results are shown in fig. 2, depicting RMSE_n as a function of the measurement noise standard deviations. As expected, the results suggest degradation in estimation performance with increasing noise level. However, it can be observed that MHE fairly insensitive to changes in noise levels.

TABLE I

PERFORMANCE EVALUATION FOR CONGESTED SCENARIO

meas. comp.	TTS ($\times 10^7$ veh·s)	RMSE_n (veh)	RMSE_q (veh/s)	mean/max CPU time of MHE+MPC (s)
no control	6.56	-	-	-
h_1	4.55	163.6	0.08	0.76/0.98
h_2	4.54	270.5	0.90	0.75/1.00
h_3	4.40	126.1	0.08	0.74/0.96
h_4	4.42	215.4	0.82	0.74/1.01

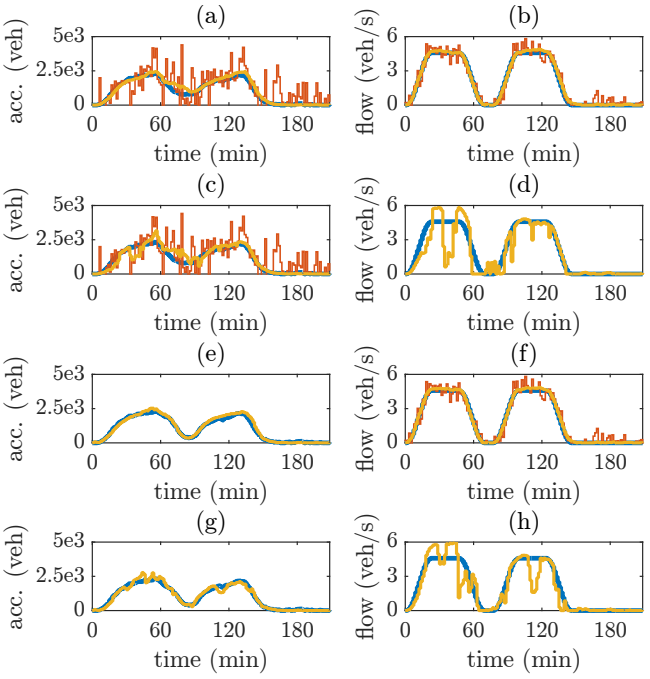

Fig. 1. Congested scenario results of the MHE-MPC scheme with the four measurement compositions, showing the true (blue), measured (red), and estimated (yellow) values of $n_{12}(t)$ ((a)-(c)-(e)-(g)) and $q_{12}(t)$ ((b)-(d)-(f)-(h)): (a)-(b) h_1, (c)-(d) h_2, (e)-(f) h_3, (g)-(h) h_4.

V. CONCLUSION

In this paper we proposed a nonlinear MHE scheme capable of OD inflow demand and accumulation state estimation for a two-region large-scale urban network model with MFD-based dynamics, together with four practically motivated measurement compositions. Observability tests revealed that observability is retained for compositions with limited or no measurements on OD-based information. This has practical significance, since OD-based measurements are usually not available or difficult to obtain in real-time. Future work could include more detailed sensitivity analyses and comparisons with traditional methods such as the extended Kalman filter.

REFERENCES

[1] C. Diakaki, M. Papageorgiou, and K. Aboudolas, "A multivariable regulator approach to traffic-responsive network-wide signal control," *Control Engineering Practice*, vol. 10, no. 2, pp. 183–195, 2002.

[2] K. Aboudolas, M. Papageorgiou, A. Kouvelas, and E. Kosmatopoulos, "A rolling-horizon quadratic-programming approach to the signal control problem in large-scale congested urban road networks," *Transportation Research Part C: Emerging Technologies*, vol. 18, no. 5, pp. 680–694, 2010.

[3] A. Kouvelas, K. Aboudolas, M. Papageorgiou, and E. B. Kosmatopoulos, "A hybrid strategy for real-time traffic signal control of urban road networks," *IEEE Transactions on Intelligent Transportation Systems*, vol. 12, no. 3, pp. 884–894, 2011.

[4] P. Varaiya, "Max pressure control of a network of signalized intersections," *Transportation Research Part C: Emerging Technologies*, vol. 36, pp. 177–195, 2013.

[5] A. Kouvelas, J. Lioris, S. Fayazi, and P. Varaiya, "Maximum pressure controller for stabilizing queues in signalized arterial networks," *Transportation Research Record: Journal of the Transportation Research Board*, no. 2421, pp. 133–141, 2014.

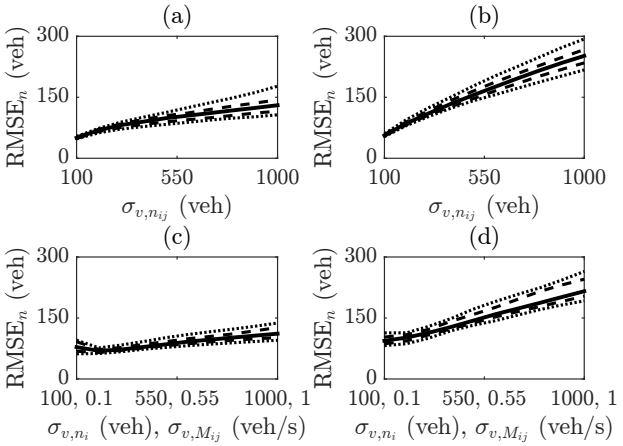

Fig. 2. Sensitivity of accumulation state $n_{ij}(t)$ estimation performance to changes in measurement noise intensity, showing the 10th and 90th (dotted), 25th and 75th (dashed), and 50th (solid) percentiles of RMSE$_n$, for a set of 50 randomly generated scenarios and the four measurement compositions: (a) h_1, (b) h_2, (c) h_3, (d) h_4.

[6] T. Wongpiromsarn, T. Uthaicharoenpong, Y. Wang, E. Frazzoli, and D. Wang, "Distributed traffic signal control for maximum network throughput," in *15th International IEEE Conference on Intelligent Transportation Systems*. IEEE, 2012, pp. 588–595.

[7] A. A. Zaidi, B. Kulcsar, and H. Wymeersch, "Traffic-adaptive signal control and vehicle routing using a decentralized back-pressure method," in *European Control Conference*. IEEE, 2015, pp. 3029–3034.

[8] X. Sun, L. Muñoz, and R. Horowitz, "Highway traffic state estimation using improved mixture kalman filters for effective ramp metering control," in *Decision and Control, 2003. Proceedings. 42nd IEEE Conference on*, vol. 6. IEEE, 2003, pp. 6333–6338.

[9] Y. Wang and M. Papageorgiou, "Real-time freeway traffic state estimation based on extended kalman filter: a general approach," *Transportation Research Part B: Methodological*, vol. 39, no. 2, pp. 141–167, 2005.

[10] A. Messner and M. Papageorgiou, "Metanet: A macroscopic simulation program for motorway networks," *Traffic Engineering & Control*, vol. 31, no. 8-9, pp. 466–470, 1990.

[11] L. Mihaylova, R. Boel, and A. Hegyi, "Freeway traffic estimation within particle filtering framework," *Automatica*, vol. 43, no. 2, pp. 290–300, 2007.

[12] Y. Yuan, J. Van Lint, R. E. Wilson, F. van Wageningen-Kessels, and S. P. Hoogendoorn, "Real-time lagrangian traffic state estimator for freeways," *IEEE Transactions on Intelligent Transportation Systems*, vol. 13, no. 1, pp. 59–70, 2012.

[13] R. Pueboobpaphan and T. Nakatsuji, "Real-time traffic state estimation on urban road network: the application of unscented kalman filter," in *Applications of Advanced Technology in Transportation*, 2006, pp. 542–547.

[14] Q.-J. Kong, Z. Li, Y. Chen, and Y. Liu, "An approach to urban traffic state estimation by fusing multisource information," *IEEE Transactions on Intelligent Transportation Systems*, vol. 10, no. 3, pp. 499–511, 2009.

[15] A. Nantes, D. Ngoduy, A. Bhaskar, M. Miska, and E. Chung, "Real-time traffic state estimation in urban corridors from heterogeneous data," *Transportation Research Part C: Emerging Technologies*, vol. 66, pp. 99–118, 2016.

[16] N. Geroliminis and C. F. Daganzo, "Existence of urban-scale macroscopic fundamental diagrams: Some experimental findings," *Transportation Research Part B: Methodological*, vol. 42, no. 9, pp. 759–770, 2008.

[17] J. Godfrey, "The mechanism of a road network," *Traffic Engineering and Control*, vol. 11, no. 7, pp. 323–327, 1969.

[18] J. Haddad and N. Geroliminis, "On the stability of traffic perimeter control in two-region urban cities," *Transportation Research Part B: Methodological*, vol. 46, no. 9, pp. 1159–1176, 2012.

[19] K. Ampountolas, N. Zheng, and N. Geroliminis, "Macroscopic modelling and robust control of bi-modal multi-region urban road networks," *Transportation Research Part B: Methodological*, vol. 104, pp. 616–637, 2017.

[20] H. Ding, Y. Zhang, X. Zheng, H. Yuan, and W. Zhang, "Hybrid perimeter control for two-region urban cities with different states," *IEEE Transactions on Control Systems Technology*, 2017.

[21] H. Fu, N. Liu, and G. Hu, "Hierarchical perimeter control with guaranteed stability for dynamically coupled heterogeneous urban traffic," *Transportation Research Part C: Emerging Technologies*, vol. 83, pp. 18–38, 2017.

[22] J. Haddad, "Optimal perimeter control synthesis for two urban regions with aggregate boundary queue dynamics," *Transportation Research Part B: Methodological*, vol. 96, pp. 1–25, 2017.

[23] A. Kouvelas, M. Saeedmanesh, and N. Geroliminis, "Enhancing model-based feedback perimeter control with data-driven online adaptive optimization," *Transportation Research Part B: Methodological*, vol. 96, pp. 26–45, 2017.

[24] R. Zhong, C. Chen, Y. Huang, A. Sumalee, W. Lam, and D. Xu, "Robust perimeter control for two urban regions with macroscopic fundamental diagrams: a control-lyapunov function approach," *Transportation Research Part B: Methodological*, 2017.

[25] J. Haddad and Z. Zheng, "Adaptive perimeter control for multi-region accumulation-based models with state delays," *Transportation Research Part B: Methodological*, 2018.

[26] N. Geroliminis, J. Haddad, and M. Ramezani, "Optimal perimeter control for two urban regions with macroscopic fundamental diagrams: A model predictive approach," *IEEE Transactions on Intelligent Transportation Systems*, vol. 14, no. 1, pp. 348–359, 2013.

[27] M. Hajiahmadi, J. Haddad, B. De Schutter, and N. Geroliminis, "Optimal hybrid perimeter and switching plans control for urban traffic networks," *IEEE Transactions on Control Systems Technology*, vol. 23, no. 2, pp. 464–478, 2015.

[28] M. Ramezani, J. Haddad, and N. Geroliminis, "Dynamics of heterogeneity in urban networks: aggregated traffic modeling and hierarchical control," *Transportation Research Part B: Methodological*, vol. 74, pp. 1–19, 2015.

[29] I. I. Sirmatel and N. Geroliminis, "Economic model predictive control of large-scale urban road networks via perimeter control and regional route guidance," *IEEE Transactions on Intelligent Transportation Systems*, vol. 19, no. 4, pp. 1112–1121, April 2018.

[30] M. Yildirimoglu, M. Ramezani, and N. Geroliminis, "Equilibrium analysis and route guidance in large-scale networks with MFD dynamics," *Transportation Research Part C: Emerging Technologies*, vol. 59, pp. 404–420, 2015.

[31] R. Hermann and A. Krener, "Nonlinear controllability and observability," *IEEE Transactions on Automatic Control*, vol. 22, no. 5, pp. 728–740, 1977.

[32] H. G. Kwatny and G. Blankenship, *Nonlinear Control and Analytical Mechanics: A Computational Approach*, ser. Control Engineering. Birkhäuser Basel, 2000.

[33] M. N. Chatzis, E. N. Chatzi, and A. W. Smyth, "On the observability and identifiability of nonlinear structural and mechanical systems," *Structural Control and Health Monitoring*, vol. 22, no. 3, pp. 574–593, 2015.

[34] M. Diehl, H. J. Ferreau, and N. Haverbeke, "Efficient numerical methods for nonlinear mpc and moving horizon estimation," in *Nonlinear model predictive control*. Springer, 2009, pp. 391–417.

[35] H. G. Bock and K.-J. Plitt, "A multiple shooting algorithm for direct solution of optimal control problems," in *Proceedings of the IFAC World Congress*, 1984.

[36] M. J. Risbeck and J. B. Rawlings, "MPCTools: Nonlinear model predictive control tools for CasADi (Octave interface)," 2016. [Online]. Available: https://bitbucket.org/rawlings-group/octave-mpctools

[37] J. A. Andersson, J. Gillis, G. Horn, J. B. Rawlings, and M. Diehl, "CasADi: A software framework for nonlinear optimization and optimal control," *Mathematical Programming Computation*, pp. 1–36, 2018.

[38] A. Wächter and L. T. Biegler, "On the implementation of an interior-point filter line-search algorithm for large-scale nonlinear programming," *Mathematical Programming*, vol. 106, no. 1, pp. 25–57, 2006.